

PSFC/RR-98-1

Field Test of a Real-Time Calibrated Microwave Plasma Continuous Emissions Monitor for Stack Exhaust Metals

Paul P. Woskov, Kamal Hadidi, Paul Thomas, Karyn Green,
Guadalupe Flores, and David A. Lamar¹

February 1998

*Plasma Science and Fusion Center
Massachusetts Institute of Technology
Cambridge, MA 02139*

This work was supported by the U. S. Department of Energy, Office of Science and Technology, Mixed Waste Focus Area. Reproduction, translation, publication, and use in whole or in part, by or for the United States government is permitted.

¹ Battelle, Pacific Northwest National Laboratory, Richland, Washington

Table of Contents

Technology Description	1
Development History	2
Equipment	3
<i>Sample Probe</i>	3
<i>Calibration System</i>	3
<i>Microwave Plasma</i>	4
<i>Suction Pump System</i>	5
<i>Optics</i>	5
<i>Spectrometer System</i>	6
<i>Operational Requirements</i>	6
Procedures	7
<i>Spectral Data Acquisition</i>	7
<i>Calibration Procedures</i>	8
<u>Nebulizer Calibration</u>	8
<u>Field Calibration</u>	10
<u>Wavelength Calibration</u>	12
<i>Procedure for Determination of Metals Concentration</i>	13
<i>Typical Daily Test Sequence</i>	13
Results	15
<i>Performance</i>	15
<i>Measurements</i>	16
Discussion	19
<i>Test Results</i>	19
<i>Relative Accuracy</i>	23
<i>Technology Strengths and Limitations</i>	25
Acknowledgments	26
References	26

List of Figures

Figure 1. Block diagram of the microwave plasma CEM	1
Figure 2. Calibration system	3
Figure 3. Microwave plasma hardware	4
Figure 4. Exhaust system	5
Figure 5. Instantaneous spectral in the lead spectral band showing zero drift ..	8
Figure 6. Calibration of flowmeter	11
Figure 7. Initial lead signal during shakedown testing	12
Figure 8. Typical daily sequence flow diagram	14
Figure 9. Detection limit vs. response time	15
Figure 10. Raw data at start of first test Sept. 22 th	16
Figure 11. Two-second smoothed lead data for 18 th test	17
Figure 12. Data for first reference method test with one minute smoothing....	18
Figure 13. Difference between the R-TiC CEM and reference method	24

List of Tables

Table 1. Operational Requirements	7
Table 2. R-TiC CEM Measured Average Metals Concentrations	20
Table 3. Lead Results	21
Table 4. Chromium Results	22
Table 5. Beryllium Results	23
Table 6. t-values	24
Table 7. Relative Accuracies	25

Abstract

A real-time calibrated microwave plasma continuous emissions monitor was installed on the exhaust stack of rotary kiln incinerator at the Environmental Protection Agency (EPA) National Risk Management Laboratory in Research Triangle park, North Carolina for trace metals monitoring tests over approximately a two week period in September 1997. This report describes the details of the hardware used for this test, measurement procedures, and results. The plasma was sustained in a shorted waveguide with a 1.5 kW, 2.45 GHz magnetron source for atomic emission spectroscopy. An undiluted stack gas sample was isokinetically drawn at 13 liters per minute by a short sample line and continuously injected into the plasma at the stack gas flow velocity of approximately 7.9 m/sec. The plasma was sustained in the undiluted stack exhaust gas and the air used for swirl flow. A real-time calibration system that could momentarily, on command, inject a known concentration of metals into the sample line was attached to a branch in the line just outside the stack. This span signal was used to maintain accurate measurements of metals concentrations for all conditions during operation. Three hazardous metals were monitored, lead, chromium, and beryllium. The measurements were referenced to two EPA Method-29 measurement locations up stream of the microwave plasma monitor. A total of twenty spiked stack exhaust tests were carried out. Ten one-hour tests at high concentration (40-60 $\mu\text{g}/\text{actual m}^3$) and ten one and half-hour tests at low concentration (10-15 $\mu\text{g}/\text{actual m}^3$). The time lengths of the tests were determined by requirements of EPA Method 29 to collect measurable metals samples. The microwave plasma generally remained on continuously for 10 to 12 hours each test day. It operated robustly in the high temperature stack environment. The microwave plasma monitor achieved measurement accuracies of approximately 20% for lead and beryllium and 40% for chromium. The data suggests that the accuracies may be even closer to the EPA reference method due to a perturbation in the stack metal concentrations between the location of the microwave plasma and where the EPA methods took their samples.

Field Test of a Real-Time Calibrated Microwave Plasma Continuous Emissions Monitor

Paul P. Woskov, Kamal Haddidi, Paul Thomas, Karyn Green, Guadalupe Flores, and
David A. Lamar¹

*Plasma Science and Fusion Center
Massachusetts Institute of Technology*

Technology Description

The real-time calibrated microwave plasma continuous emissions monitor (R-TiC CEM) uses microwave power at the household oven frequency of 2.45 GHz to sustain a plasma in a flowing sample of the exhaust stack gas for atomic-emission-spectroscopy (AES) of entrained metals. The plasma hardware is mounted onto the exhaust stack and an undiluted sample of the exhaust gas at stack flow velocity is continuously directed into the plasma chamber by a short sample line. The continuous volume of stack gas sampled in the range 10-30 l/min is similar to that sampled by the current EPA standard Method-29, but through a shorter sample line. Near *in situ* installation of the microwave plasma minimizes metals and particulate transport losses and provides access to the plasma for field calibration. Another advantage of having the plasma just outside the stack rather than inside is that the plasma parameters and light collection can be optimized for maximum sensitivity unlike *in situ* plasma spark systems.

The major elements of the R-TiC CEM and their configuration are illustrated in Figure 1. A short sample line directs a fraction of the stack gas to the microwave plasma. The sample line has a branch just outside the stack that is connected to a calibration system that periodically, on command, adds a known metal concentration to provide a real-time span calibration. The microwave plasma volatilizes all particulates, breaks up species into their elemental components, and excites atomic emission. A suction pump system establishes an isokinetic draw of the stack gases into the plasma and returns these gases back to the stack downstream from the sample line. Optics collect the plasma emission light by a longitudinal view down the axis of the plasma column and focus this light onto short fused quartz fiber optic cables for transmission to one or more spectrometers. The spectrometer resolves the atomic emission spectra for detection. Computers identify the relevant metal emission lines and record and display the signal levels in real-time. The signal levels are proportional to the metals concentrations in the plasma.

Development History

Initial laboratory tests of an air microwave plasma for metals detection were carried out at the Massachusetts Institute of Technology (MIT) in 1993. The Office of Science and Technology, Department of Energy (DOE) supported this work as part of a project to develop graphite electrode DC plasma arc technology for the treatment of

¹ Pacific North West National Laboratory

mixed DOE wastes. A number of advanced diagnostics were needed for this project including sensors for heavy metals emissions. The 1993 experiments demonstrated robust plasma operation in air and high sensitivity to mercury vapor with a limit of detection equal to approximately $3 \mu\text{g}/\text{m}^3$ in slow nitrogen and air gas flows [1].

In the following two years more extensive testing was carried out. Continued laboratory testing confirmed the robust nature of the microwave plasma including the ability to operate with gas flows having large particulate and moisture loadings. High sensitivity, ranging from 0.04 to $3 \mu\text{g}/\text{m}^3$ was demonstrated for 10 of the Resource Conservation and Recovery Act (RCRA) metals when salts of the metals were directly inserted into the plasma [2]. Laboratory tests at PNNL also demonstrated an initial detection limit of approximately $17 \mu\text{g}/\text{m}^3$ for plutonium [3].

Following the successful laboratory tests, a microwave plasma device constructed entirely of refractory materials was installed into a pilot scale arc furnace exhaust duct at MIT, where temperatures reached $664 \text{ }^\circ\text{C}$ ($1227 \text{ }^\circ\text{F}$). It operated continuously for 49 hours, providing qualitative measurements of chromium, manganese, and iron, with 0.5 second time resolution [2]. Some preliminary qualitative testing was also carried out in a radioactive furnace environment at PNNL.

In the past year the emphasis of the development activity has focused on calibrated, quantitative measurements and on improving metals sensitivity for fast aerosol flows. After some initial work with dry powder feeding, a pneumatic nebulizer was configured for real-time injection of calibrated aerosol samples during operation of the R-TiC CEM on a furnace stack. The September 1997 test at the EPA National Risk Management Laboratory represents the first time that the R-TiC CEM technology has been used for quantitative measurements on a furnace. The Mixed Waste Focus Area, Office of Science and Technology, DOE, currently supports this work.

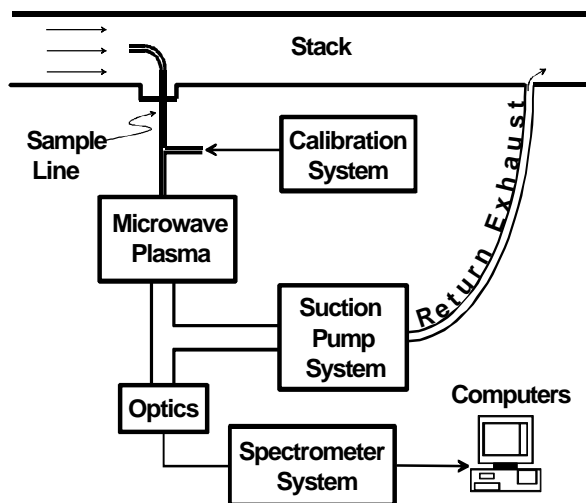


Figure 1. Block diagram of the microwave plasma continuous emissions monitor

Equipment

Sample Probe

The sample probe used for the EPA test was a 35 cm long, 6 mm internal diameter fused quartz tube with a 90° bend, 50 mm radius, which intercepted the gas flow in the center of the 203.2 mm diameter stack and directed it out the side port. Being just a bare quartz tube it was brought out of the stack through a standard 7.938 mm (5/16 inch) vacuum feed through on the port flange.

The original design for interfacing this probe to the plasma was to use a ball and socket joint to connect it to the 19 cm long, 6 mm i.d. quartz tube tee going into the plasma chamber. The ball and socket joint would allow some motion between the stack and the microwave plasma hardware without breaking the sample probe. The total sample line length from the center of the stack to the plasma chamber in this case would have been approximately 57 cm. However, because of the precarious positioning of the plasma hardware on a swaying scaffold 14 feet above ground level, much larger motions occurred between the microwave plasma hardware and stack than had been anticipated. This necessitated the replacement of the ball joint section with a 1 m long flexible loop of 7.938 mm (5/16 inch) diameter Teflon tubing. The total sample line length was thus increased to 151 cm for the EPA test even though the plasma hardware itself was only approximately 30 cm away from the stack port.

The continuous gas volume delivered to the plasma chamber by this sample probe corresponded to 13 liters per minute for an isokinetic sampled gas velocity of 7.92 m/sec (26 ft/sec).

Calibration System

The real-time span calibration system was connected to the quartz tube tee between the sample probe and the plasma chamber. The major elements of the calibration system are shown in Figure 2. A spray chamber with a Meinhard nebulizer [4] was connected to the 7.5 cm long branch tube of the tee. A Masterflex C/L peristaltic pump connected to the liquid input of the nebulizer delivered a weak nitric acid standard solution prepared by Alfa Aesar containing 200 µg/ml of each metal being quantitatively monitored. The pressurized nitrogen gas flow to the nebulizer was controlled

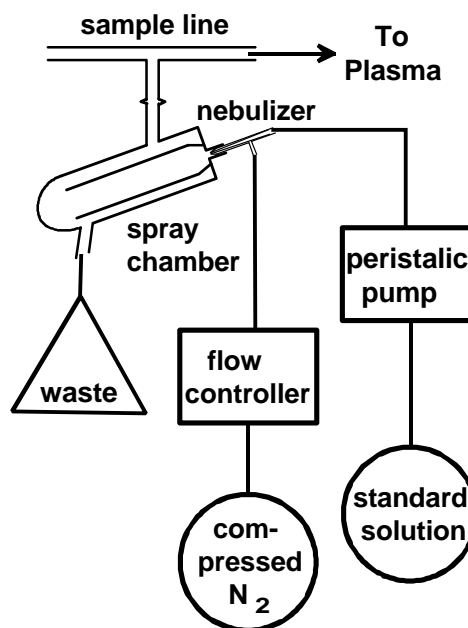


Figure 2. Calibration system.

by a MKS Instruments flow controller at a rate of 1 liter per minute. The resulting liquid feed rate into the nebulizer was 1.17 ml/min. Since the nebulizer efficiency for small aerosol droplets that get aspirated into the sample line is very low, most of the standard solution liquid is collected in a waste flask. The tubing connection to the waste flask must be air tight because it is part of the stack vacuum.

Microwave Plasma

The microwave plasma system is illustrated in Figure 3. The microwave power source was an ASTeX Model AX 2050 2.45 GHz Microwave Generator operated at a nominal forward power of 1.5 kW. A waveguide circulator protected the magnetron source from reflected power by deflecting reflected microwaves into a water-cooled dump. During the EPA testing, nominal reflected power was approximately 100 Watts. A triple stub waveguide tuner was used to match the waveguide impedance between the microwave source and plasma. The waveguide size was standard WR-284 (76.2 mm x 38.1 mm (3.0 inch x 1.5 inch) outside dimensions) which is normally used for the next higher frequency band. However, in our application this smaller waveguide size increased the microwave power density for improved plasma robustness. A window between the plasma and triple stub tuner served as a vacuum seal to the stack and kept the circulator and magnetron clean.

The waveguide section in which the plasma is sustained is tapered in width to 76.2 mm x 19.05 mm (3.0 inch x 0.75 inch) to further increase the microwave power density. A 25.4 mm i.d. boron nitride tube penetrates through the center of the wider waveguide walls one quarter wavelength back from the shorted end of the waveguide. The plasma is sustained inside this boron nitride tube. The gas-input side of the boron nitride tube is

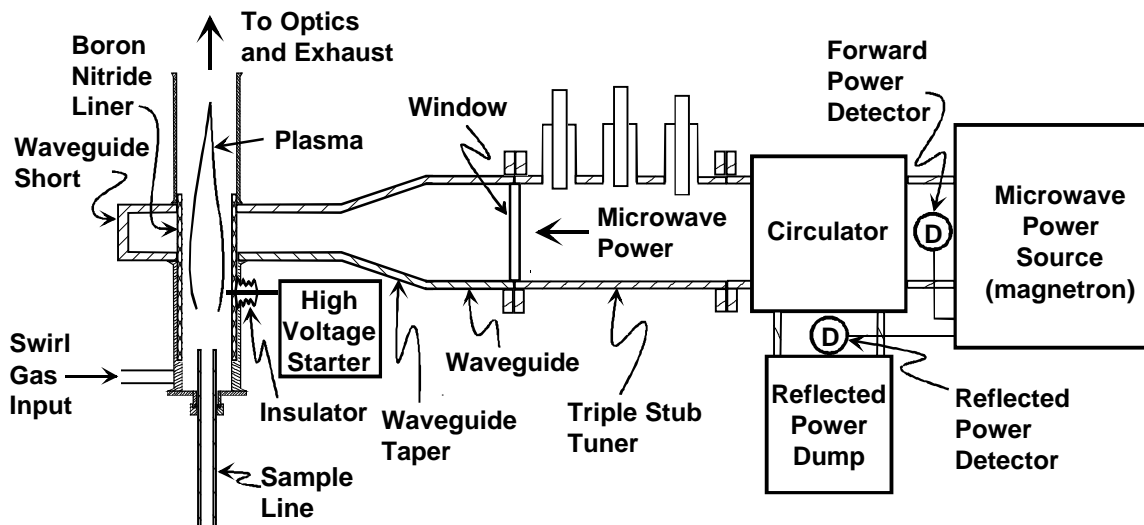


Figure 3. Microwave plasma hardware.

capped with a 7.938 mm (5/16 inch) vacuum feed through for the sample line. The sample line enters into the center of the boron nitride tube and terminates approximately 100 mm back from the base of the waveguide. Swirl gas is also injected at the entry location of the sample line to keep the plasma centered. The swirl gas has replaced the central dielectric tube used previously [2] for plasma centering because the dielectric tube was prone to failure due to thermal stresses. Air was used as the swirl gas for the EPA test. A high voltage spark near the base of the waveguide is used to start the plasma. The plasma generally extends approximately 100 mm or more beyond the waveguide toward the optics and exhaust. For the EPA testing the plasma axis was oriented horizontally.

Suction Pump System

The suction pump system was comprised of a heat exchanger, small particle filters, an electrical pump, a valve for adjusting suction, and a flowmeter. Figure 4 illustrates the configuration of these components. The gases from the plasma first passed through a water-cooled heat exchanger to reduce the gas temperature down to the operating range of the pump. A small particle filter, Wilkerson Model E16-03-000B C97, was used in line

between the heat exchanger and the pump to protect the pump from contamination. The pump was a Cole-Parmer model GX-07055-04 rotary valve oil pump. Two additional filters, of the same type as used at the pump input, were used at the output to filter out pump oil. The

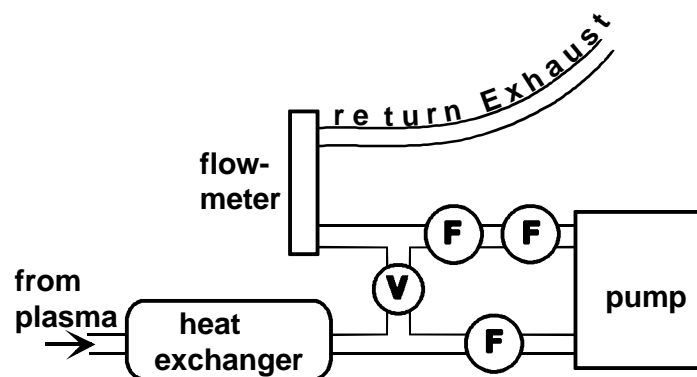


Figure 4. Exhaust system, V: valve, F: filter.

plasma gases were returned to the stack through a flowmeter, an Omega Model FL-1501A Rotameter. A bypass valve between the pump input and output was used to adjust suction for isokinetic sampling while letting the pump operate under a constant load.

Optics

To allow transmission of UV light the plasma light collection optics used fused quartz for the window, focusing lens, and fiber. The window sealed the stack and plasma vacuum envelope and provided a view down the axis of the plasma. A small gas jet continuously blew clean air onto the inside surface of the window to prevent deposition

of fly ash. The focusing lens immediately outside the window had an f-number of 3. The focused light was bifurcated by a first surface aluminum mirror inserted into the beam such that half the light was reflected to one fiber and the other half was transmitted to a second fiber. Each fiber was a single 1 mm diameter strand. The fiber cable lengths were 2 and 3 meters.

Spectrometer System

Two grating spectrometers were used to perform the AES for the EPA test. These were located on the scaffold shelving immediately below the microwave plasma hardware. One spectrometer was a commercial unit, an Instruments SA Jobin Yvon Spex Model THR-640, 0.64 m Czerny-Turner spectrometer with a 2400 groove/mm grating. It was used with a Princeton Instruments Model IRY-512W intensified 512- element diode detector array. The spectrometer spectral resolution was approximately 0.04 nm in the UV with the input slit adjusted to a minimum value of approximately 10 μm . This spectrometer was set to observe the 234.9 nm beryllium emission line.

The second spectrometer was built at MIT. It used a 3600 groove/mm grating with an output focal length of up to 0.86 m for four high resolution, non-contiguous spectral bands. Two of the bands were used during the EPA test. One band monitored chromium at 359.349 nm and the other monitored lead at 405.787 nm. Each band used a linear 2048 element CCD detector array from StellarNet, Inc. The spectral resolution was estimated at approximately 0.05 nm with a 50 μm fixed slit. Iron lines were also observed in these bands but did not interfere with the chromium and lead lines used for quantitative measurements.

A personal computer was dedicated to each spectrometer to record and display atomic emission signals in real-time. Each computer was programmed with software obtained from the detector vendors for detector operation and data acquisition. The software packages were Spectroscope from StellarNet, and CSMA from Princeton Instruments. A limited amount of real time signal processing was accomplished with this software to obtain weak metals emission signals in the presence of strong background plasma light emission. Data were recorded approximately 5 times per second with the StellarNet detectors and 2 times per second with the Princeton Instruments detector.

Operational Requirements

The operational requirements for electrical power, cooling water, and gas supplies for the real-time calibrated microwave plasma continuous emissions monitor are given in Table 1.

Table 1. Operational Requirements

Requirement	For	Value
Electrical Power	Microwave Source	408 V, 3 phase, 10 A
	Suction Pump	115 V, 1 phase, 2.2 A
	Calibration System	115 V, 1 phase, 1 A
	Spectrometers/Computers	115 V, 1 phase, 5 A
Water	Heat Exchanger	2 gal/min.
Clean Air	Plasma Swirl Flow	14 l/min.
	Optics Window	14 l/min.
Nitrogen Gas	Calibration System	1 l/min.

Procedures

Spectral Data Acquisition

A background spectrum without metals feed into the stack exhaust was first recorded for each of the metal spectral bands. The detector software automatically subtracted this background spectrum from all subsequent spectra. Figure 5 illustrates this processing step for the lead band where background emission in the air plasma is quite prominent. The top curve shows the raw spectrum and the bottom curve is the same spectrum with the background subtracted. The span calibration metals feed was on for this data set. The emission light due to the lead is not clearly observed unless the background is subtracted. This was also true for chromium and beryllium.

In addition to subtracting the background light, the software was also programmed to automatically subtract the average baseline level as determined by groups of detector pixels on either side of the metal emission line pixels. This processing step is necessary because the background plasma light emission can change slightly over the course of a one-hour or longer test, causing the subtracted background level to drift from zero. The displayed and recorded metals concentration signal, C , was therefore determined by the equation:

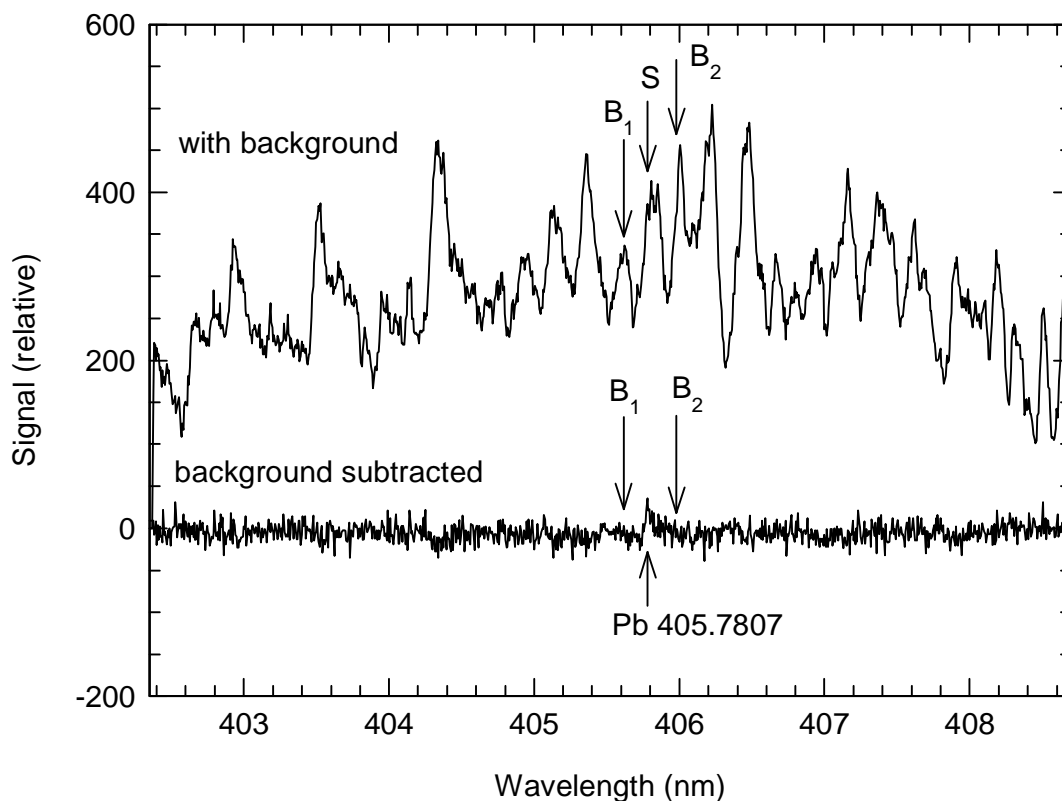


Figure 5. Instantaneous spectra in the lead spectral band illustrating background subtraction.

$$C = S - \frac{(B_1 + B_2)}{2} \quad (1)$$

where S is the signal from the metal emission line pixels and B_1 and B_2 are the signal levels from the same number of pixels on either side of the metal emission line as illustrated in Figure 5. Typically five pixels were used for each of S , B_1 , and B_2 .

Calibration Procedures

Nebulizer Calibration

The efficiency with which the nebulizer forms aerosol from the standard solution and transports metal-containing droplets to the microwave plasma chamber is the key parameter that must be known to calibrate the R-TiC CEM. This parameter was not definitely determined prior the present EPA test and is the subject of continuing research. However, upper and lower limits were established in the laboratory which combined with the initial observations of the furnace metals feed during shakedown testing in the week

prior to the reference measurements allowed the selection of a value which proved accurate in the subsequent testing.

A number of different approaches to determine the nebulizer aerosol formation and transport efficiency were attempted in the laboratory prior to the EPA test. The first and simplest was to compare the collected waste liquid volume to that which was aspirated from the uptake reservoir. The assumption here is that all the analyte corresponding to the solution volume that is missing in the collected waste is injected into the plasma. This assumption has been shown not to be accurate [4]. Not all the analyte corresponding to the missing solution volume finds its way to the plasma so this method can only establish an upper limit to the nebulizer aerosol formation and transport efficiency. Averaging six trials we determined an upper limit for the efficiency to be $5.3 \pm 1.2\%$ by this approach.

The method generally recommended for establishing the aerosol formation and transport efficiency of a nebulizer is to install a filter in the output of the plasma chamber, with the plasma off, and collect all the aerosol formed and transported through the system. The filter is then analyzed for the analyte making it through the system. In our attempts to implement this approach, we found that the filter we used obstructed the pump suction to such a degree that gas flows through the system could not be established anywhere near the operating values. Therefore we abandoned this nebulizer calibration approach.

The third nebulizer calibration method we used, and which we believe will eventually lead to a definitive calibration, measured the light emission from a directly inserted sample mass. A small droplet of the standard solution was micro-pipetted onto the tip of an alumina rod, allowed to dry, and then inserted near the base of the plasma. The resulting light signal was integrated over time as all the sample mass was volatilized. Next, the nebulizer feed time required to produce the same integrated signal was determined. Taking the ratio of the directly inserted mass to the analyte mass fed through the nebulizer to produce the same emission signal gives the aerosol formation and transport efficiency.

The advantage of this approach is that the entire R-TiC CEM system is operating exactly as it would for stack measurements except for an alumina rod that is inserted up the center of the quartz tee or through one of the high-voltage starting wire holes. The perturbation caused by inserting a blank rod was determined to be small and easily corrected for.

The main difficulty with this approach is that, to completely volatilize the solid sample, the inserted rod must be much closer to the plasma than the end of the sample line. Because there may be additional aerosol transport losses between the end of the sample line and the point of volatilization of the directly inserted mass, the nebulizer aerosol formation and transport efficiency determined by this method is a lower limit.

Also, direct insertion has the additional advantage of a longer plasma residence time for analyte vaporization from the stationary sample at the end of the insertion rod.

The nebulizer aerosol formation and transport efficiency was found to depend on the distance of the inserted sample from the plasma. A 5% nitric acid solution was used with a 200 µg/ml lead concentration and 2 µl droplets on the alumina rod. At distances of 6 mm, 16 mm, and 25 mm upstream from the waveguide wall, the efficiency was found to be $0.035 \pm 0.008\%$, $0.14 \pm 0.06\%$, and $0.35 \pm 0.08\%$, respectively. At distances greater than 25 mm upstream, the plasma heat radiation was not sufficient to completely volatilize the lead sample. The sample line output was approximately 100 mm upstream from the waveguide wall. As expected, the mass transport efficiency of the nebulizer relative to rod insertion increases as the point of rod volatilization approaches the location of the sample line gas flow output. Future research will use lower melting point metals and/or a heated filament to launch a known sample mass at the approximate location of the sample line output to better establish a calibration of the nebulizer efficiency for quantitative CEM measurements.

This calibration, of course, assumes that the efficiency of the plasma to produce light is the same for the aerosol transported calibration sample as for the vapors and particulates in the stack exhaust. Additional factors that could effect plasma light efficiency include wet versus dry particulates and the transport of slow moving versus fast-moving particulates. Additional research will be required to test these assumptions.

At the time the R-TiC CEM equipment was shipped to the EPA test site the laboratory measurements established the efficiency of the calibration nebulizer to be between the limits of 0.35 % and 5.3 %. It was also known that past determinations of the efficiency of this type of Meinhard nebulizer were between 0.5 and 1.5 % [4].

Field Calibration

The required calibration in the field must be in terms of concentration ($\mu\text{g}/\text{m}^3$). Therefore, in addition to the nebulizer mass transport into the sample line, the volume of gas into which the calibrated mass is injected must be known. To accomplish this, the flowmeter in the suction pump system was calibrated in terms of the actual sample line flow. A Matheson Model 605 flowmeter with a stainless steel ball was attached to the quartz tee input where the sample line would be connected and laboratory air was drawn through it. The Matheson flowmeter readings were recorded as the suction system valve was adjusted. The R-TiC CEM was operated as it would be for stack measurements for this sample line flow calibration. The results are plotted in Figure 6. The vertical axis corresponds to the Matheson flowmeter reading in terms of airflow at standard temperature and pressure (the approximate condition for this calibration) and the horizontal axis corresponds to the output flowmeter reading. The measurements were made for two different swirl flow settings covering the range of actual operation during the EPA reference measurements. To establish isokinetic sampling, the sample line had to be set at an actual flow of approximately 13 l/min.

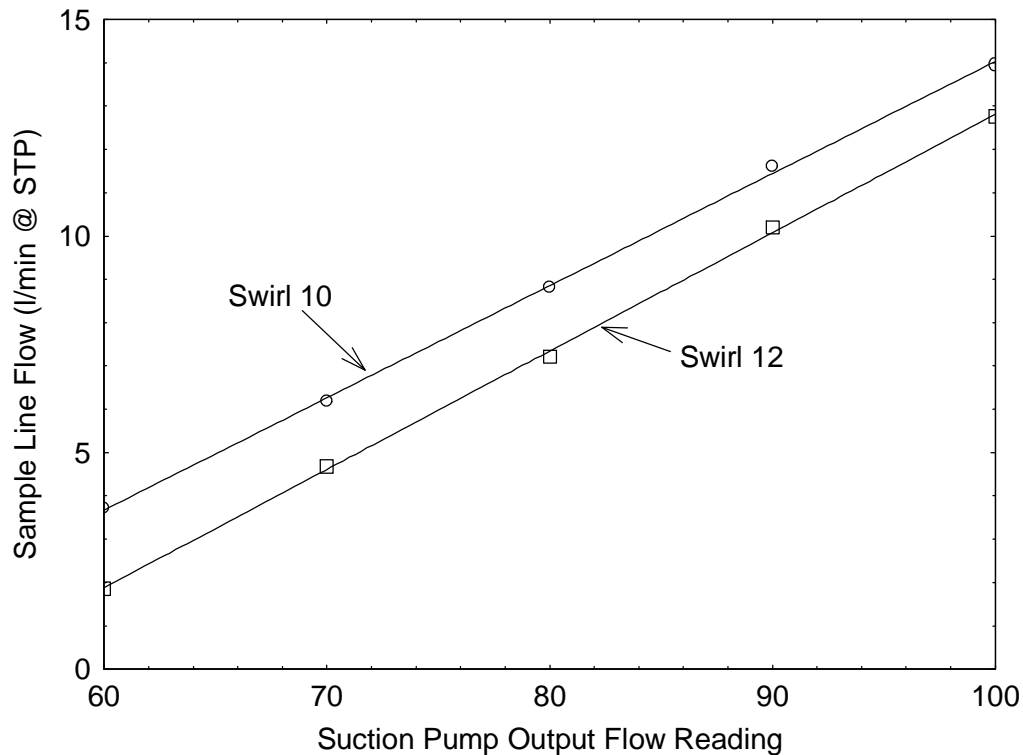


Figure 6. Calibration of suction pump system flowmeter for sample line flow.

The initial field observations of the EPA stack metals feed was used to determine the calibration nebulizer mass transport efficiency. Part of the data for lead on the afternoon of September 19th, the week before the reference measurements, is shown in Figure 7. The point at which the aerosol metals feed to the furnace was turned off is marked near the middle of the plot. The dashed line through the signal level after the metals feed was turned off denotes the zero metals baseline. The signal level before the metals are turned off corresponds to the concentration of lead present in the stack, except for a one and a half-minute period approximately 14 minutes into the data set when the calibration nebulizer was turned on. The test operators stated at the time that the stack lead concentration was in the range of 20 - 30 $\mu\text{g}/\text{acm}$. The nebulizer mass transport efficiency would need to be 0.50% with the above determined sample line gas volume flow to be consistent with this data. This number was also consistent with the laboratory limits and was therefore adopted for all R-TiC CEM measurements during the following week. The nebulizer transport efficiency is actually somewhat higher if the gas volume flow is corrected for temperature.

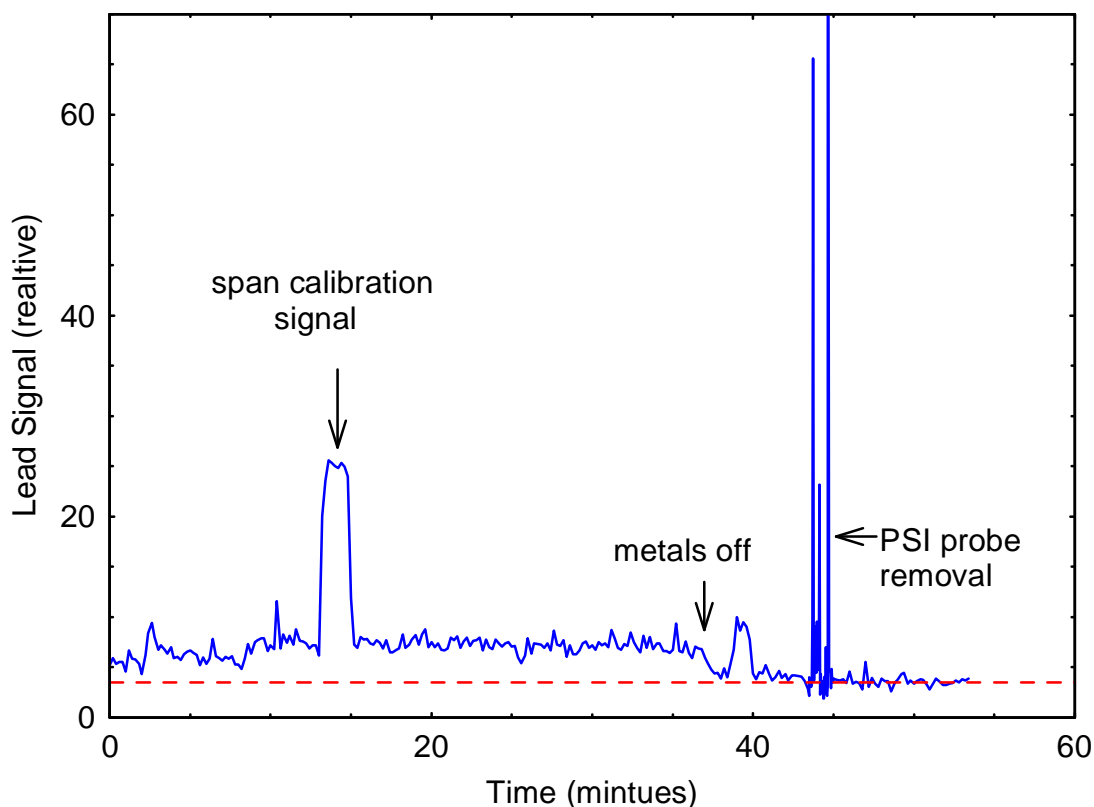


Figure 7. Initial lead signal data during shakedown testing on the afternoon of Sept. 19th.

Additional features in the metals signals first noted during the shakedown testing were large transients whenever hardware changes were made to the stack. In particular, the PSI probe*, which was installed at the beginning of each day's testing and removed at the end of each day, generated signal-saturating metals concentrations every time it was removed as shown in Figure 7. This probe was a large aluminum tube inserted halfway into the stack, a cold finger that occluded approximately 20% of the stack cross-section just upstream of the R-TiC CEM. We believe a small fraction of the metals deposited onto this probe during a day's testing were blown off each time it was removed. Another stack flange opening event upstream from the PSI probe produced the bump in the signal at 39 minutes just after the metals were turned off. The time resolution for the data in Figure 7 is 12 seconds except in the vicinity of the PSI transients where it is 2.4 seconds.

Wavelength Calibration

The spectrometer detector array pixels corresponding to the metal emission lines being monitored were determined by turning on the calibration nebulizer and taking a spectrum for each spectrometer band as shown in Figure 5 for lead. Each metal being monitored was present in the standard solution and the desired metal emission lines were

* An *in situ* electric spark system also being tested for multi-metals monitoring just upstream of the R-TiC CEM.

readily evident when the nebulizer was turned on. The detector pixels corresponding to the desired metals and background for analysis of Equation 1 were identified and programmed into the equation. The wavelength calibration was checked at the beginning of each day's testing and occasionally during the day. Some wavelength drift was noted. For the MIT constructed spectrometer this drift was not significant and would not preclude continuous emissions measurements throughout the test period if left uncorrected. However, we did optimize the pixel setting if a change was noted. For the ISA spectrometer, the wavelength drift was more significant and required correction during the course of a day's testing. Activating a cooling loop installed in the Princeton Instruments detector array would eliminate this drift in the future.

Procedure for Determination of Metals Concentrations

The procedure for the determination of the metals concentrations is easily understood by referring to Figure 7. For each of the 10 high concentration tests and 10 low concentration tests a data set similar to Fig 7 was recorded showing the metals signal with the metals feed on, metals feed off, and span calibration signal. The fly ash contribution, which was continuously present throughout the data sets, could be distinguished as brief transients at the raw data time resolution of 0.2 seconds. These transients could therefore be ignored in the zero and span level determinations. Using the known concentration (200 $\mu\text{g/ml}$) and uptake rate (1.17 ml/min) of the metals standard solution, a nebulizer efficiency of 0.5%, and the measure volume of gas flow (13 l/min) in the sample line, the nebulizer span signal corresponds to a concentration of 92 $\mu\text{g/acm}$. The metals concentration corresponding to the stack exhaust signal is simply the ratio of this signal to the span signal times 92 $\mu\text{g/acm}$.

Typical Daily Test Sequence

The typical daily test sequence is outlined in the flow diagram in Figure 8. A test day began with turning on the R-TiC CEM system approximately one hour before the stack metals feed was started. The cooling water and suction pump were started first, followed by start up of the microwave plasma with the high-voltage spark. Finally, the swirl and window gas flows were turned on. Once plasma light emission was established, background spectra were stored for automatic subtraction from subsequent emission measurements. The emission wavelengths were checked next by briefly turning on the nebulizer. The data acquisition detector pixel numbers were adjusted in the software if necessary. The data acquisition was then started to record the metals signals, preferably before the stack metals feed was started to get an initial zero level check.

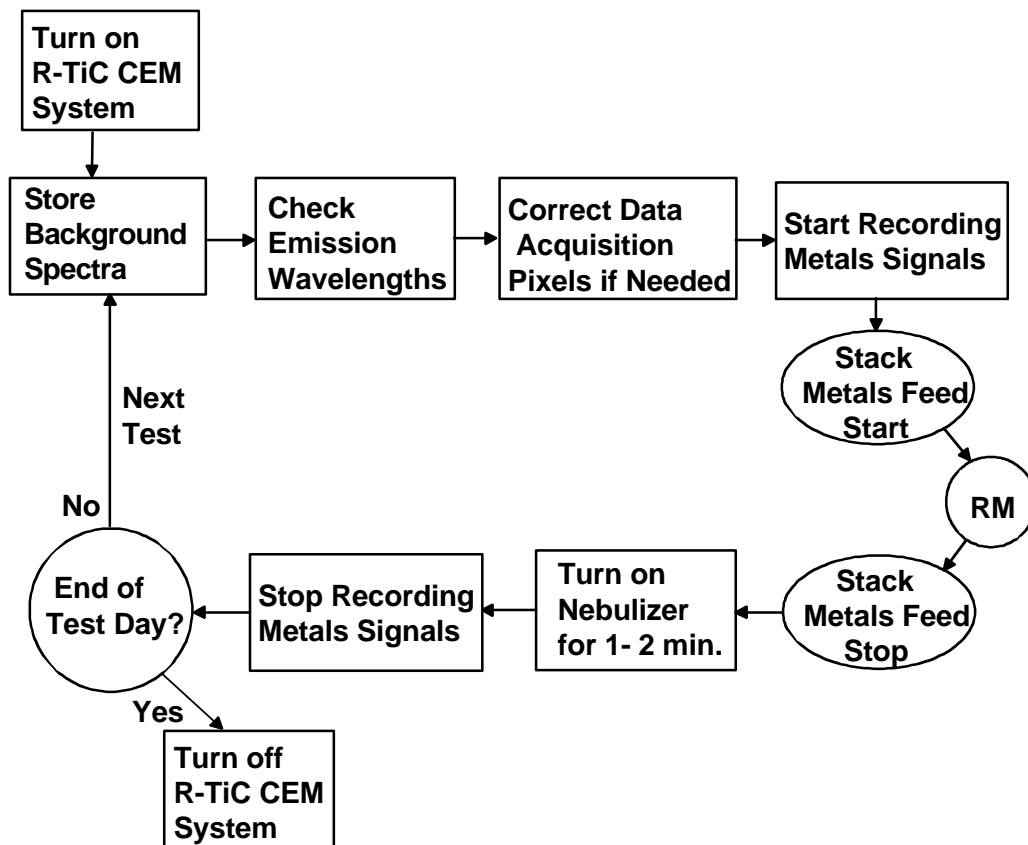


Figure 8. Typical daily sequence flow diagram.

After the reference measurements and metals feed were stopped, the R-TiC CEM data acquisition continued to acquire a zero level. Then the nebulizer was turned on for one to two minutes to provide a calibration span check. Once the zero and span data were acquired, data recording was stopped. If another test was to follow, the test sequence was restarted with the storing of new background spectra. If the test day was over, then the R-TiC CEM system was shut down.

The flow diagram is typical; some variations occurred during the one week test period. It was not necessary to check the wavelengths between every test, particularly late in the day when equipment drifts were negligible. Also the calibration nebulizer was turned on more often than once during some of the tests to get additional span calibration data. One of the advantages of this calibration method is that it can be turned on whenever and as often desired to maintain confidence in the measurements. It is essentially the method of standard additions [5].

Results

Performance

The detection limit for metals in analytical plasmas is generally defined as the concentration that yields a signal equal to three times the standard deviation of the noise fluctuations. The standard deviation for a given data set is a measure of how precisely a root mean square (rms) value can be assigned to that data set. For thermal or white noise, the standard deviation varies as the inverse square root of the signal integration time. Incoherent plasma light emission is inherently a thermal process. Therefore, detection limit and measurement times are related to each other. The lower the detection limit, the longer will be the measurement time and instrument response time.

The detection limit and its relation to the measurement time were evaluated for the data taken during the EPA test. Figure 9 shows the analysis of the signal fluctuations for the three metals monitored by the R-TiC CEM. For chromium and lead, 3.5 minute data sets of approximately 1000 points each were evaluated over a period when the signal level was relatively flat with fly ash on but no metals feed. For beryllium, a 5 minute time period of 600 points was evaluated with both fly ash and metals feed. Each of the data sets was filtered with a number of different integration

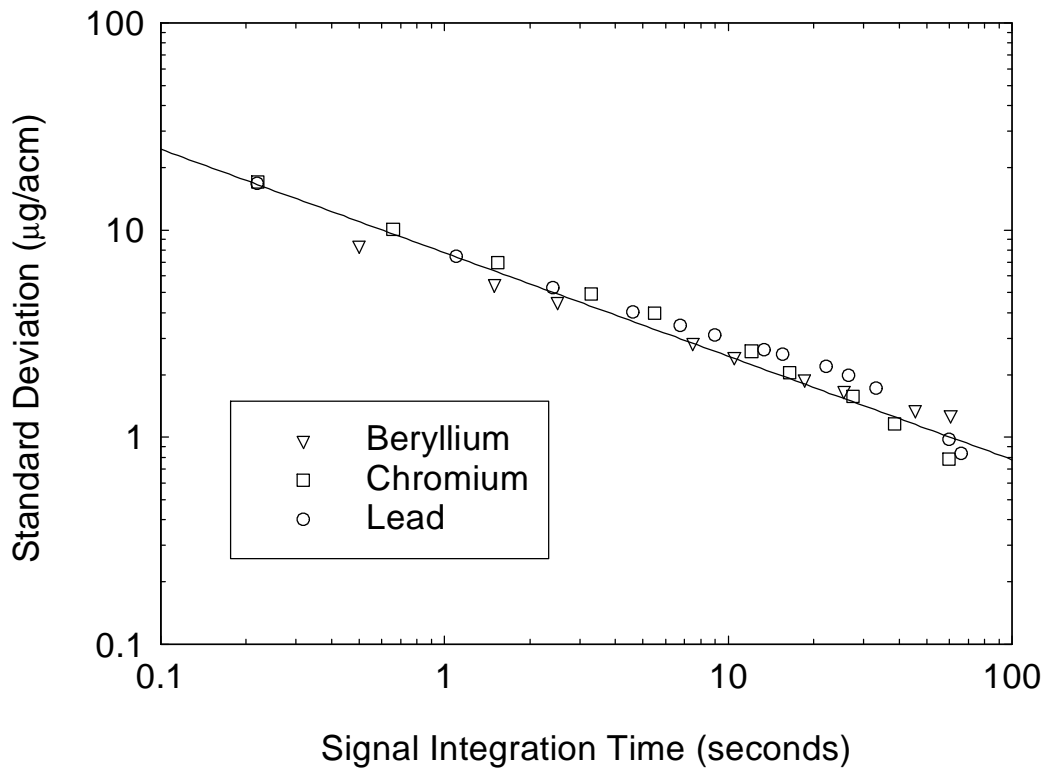


Figure 9. The relationship between detection limit (3x vertical axis) and response time.

Times (data smoothing), covering the range from 0.2 seconds to 1 minute for Cr and Pb, and 0.5 seconds to 1 minute for Be. For each integration time, the standard deviation of the resulting data set was calculated and plotted in Figure 9. The minimum integration time in each data set corresponds to the raw data time resolution. The straight line on the log-log plot is the best fit of a square root function to all the data points. There is good agreement for a white noise relationship between the standard deviation and the integration time and no evidence of a $1/F$ noise limit out to the maximum one minute integration time considered here. Taking three times the standard deviation as the detection limit, the present R-TiC CEM results show that for an integration time of 0.2 seconds the detection limit is approximately $50 \mu\text{g}/\text{m}^3$. At one minute it decreases to approximately $3 \mu\text{g}/\text{m}^3$, and it is projected to be $1 \mu\text{g}/\text{m}^3$ for an integration (measurement) time of approximately 10 minutes.

Measurements

Data were collected for lead, chromium, and beryllium. Figure 10 shows 3.5 minute long samples of raw data for lead and chromium at the beginning of the first reference measurement test on Monday morning September 22th. The notable features in the raw data are the large signal spikes caused by individual fly ash particulates. The

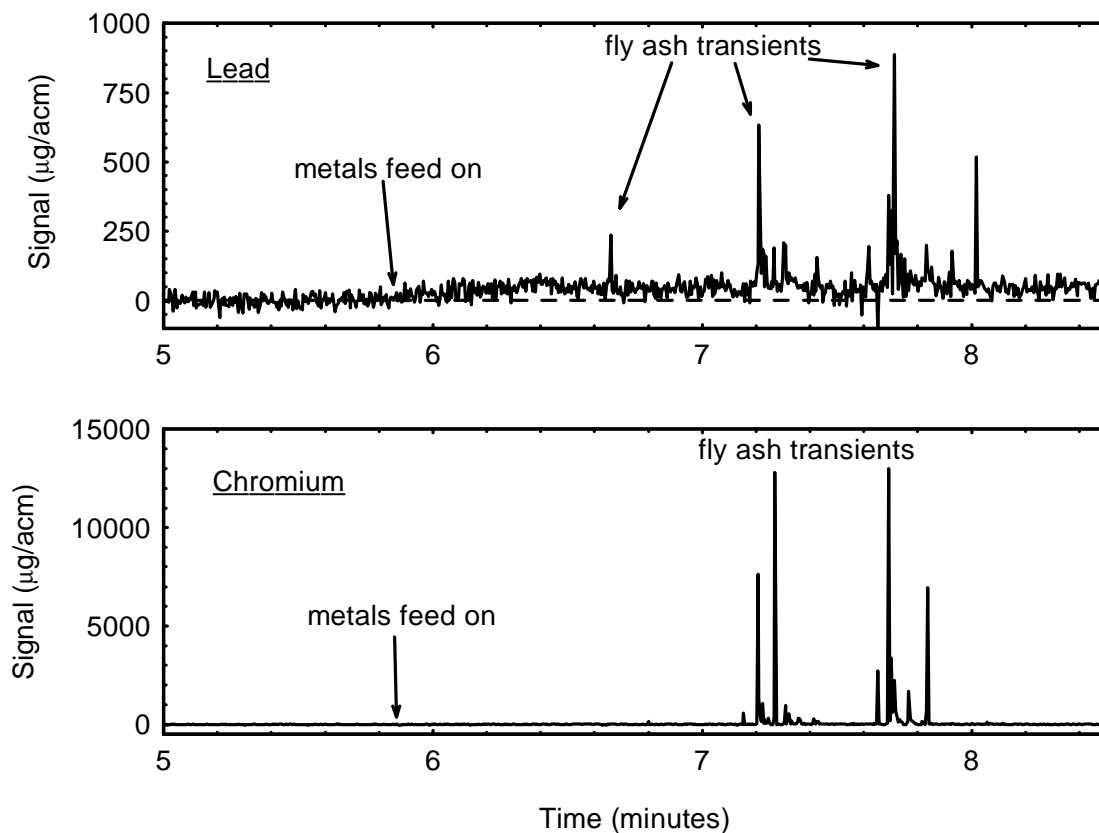


Figure 10. Raw data taken at beginning of the first reference method test Sept. 22th.

concentration scale extrapolated from the 92 $\mu\text{g}/\text{acm}$ nebulizer level indicates transient concentrations due to lead particulates of the order of 1000 $\mu\text{g}/\text{acm}$ and for chromium over 10000 $\mu\text{g}/\text{acm}$. The chemical composition of the particulates varied, some with lead, some with chromium, and others with both lead and chromium. The fly ash contained much more chromium than lead. Similar data for beryllium did not reveal any fly ash particulates with beryllium.

The raw data illustrates that the R-TiC CEM is a truly continuous monitor, collecting signal for every particulate in the sample stream at every instant of time like the reference method. However, unlike the reference method it has a much shorter time resolution. The fly ash transients could be used to determine particulate sizes and number densities as demonstrated by the Takahara et al [6], also with a microwave plasma, but for our purposes the raw signals were averaged for comparison to the reference method.

Zero drift was observed in many of the data sets despite the spectral data acquisition processing steps described on pages 7 and 8. Figure 11 illustrates this for the 18th test data set for lead, the 8th low concentration test. The data shown here was smoothed with a 2-second time resolution that significantly reduced the peak height

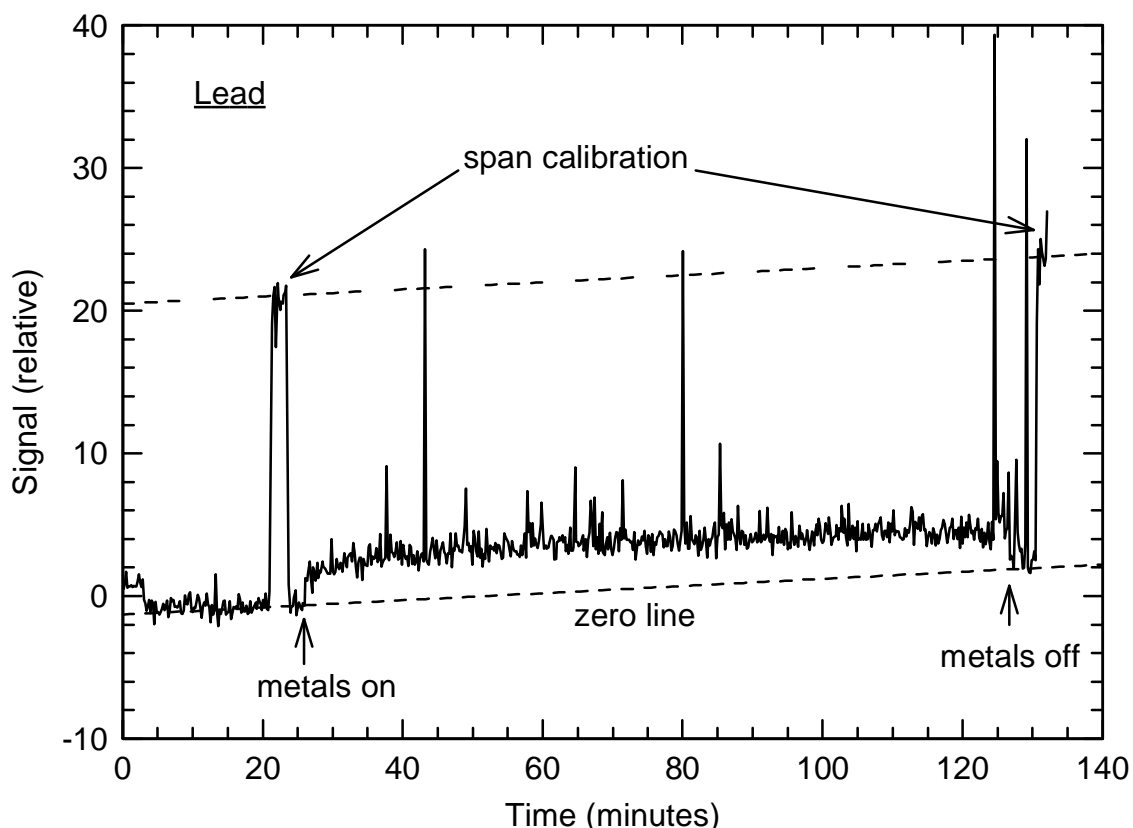


Figure 11. Two-second smoothed lead data for 18th test illustrating zero drift. of the fly ash transients. In this case a span calibration was taken at both the beginning and the end of the stack metals spiking period as shown. The zero line and span calibration level both drifted upward in parallel for this case, indicating that the system

gain or sensitivity to metals concentration was not changing. In some other data sets the drift was observed to be downward. The relative signal scale here is the same as for Figure 5. The magnitude of the drift is 2 counts over a period of 2 hours. This is small relative to the background light level, which is approximately in the range of 200 - 400 counts, but large relative to a $15 \mu\text{g}/\text{m}^3$ lead signal which is also approximately 2 counts. A slight change in the background light levels during the course of a measurement was the probable cause of the observed drift. For the present tests the drift could be readily corrected for by observing the zero line before and after a stack metals spiking run. However in the future, practical implementations of this CEM will require improvements in the data acquisition analysis and/or a method for doing a zero check in real time.

Figure 12 shows the complete data records for Pb and Cr corrected for zero drift and smoothed with a 1-minute integration time (resolution) for the time period overlapping reference method test #1. These plots are representative of the results seen

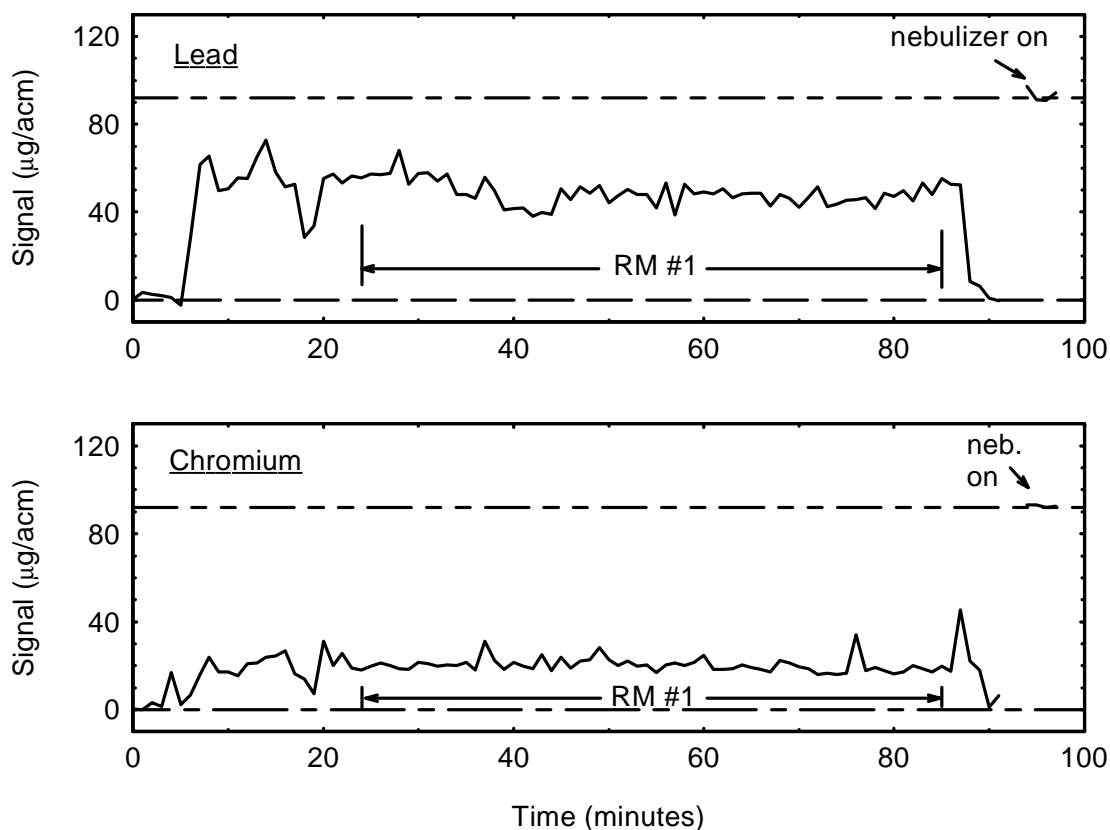


Figure 12. Data for first reference method test with one-minute smoothing.

in all the tests. The turn-on and turn-off of the aerosol metals feed into the furnace is clearly evident by the stepped increase and decrease of the metals signals at the beginning and end of each record, at approximately 6 and 89 minutes, respectively in Figure 12. The calibration nebulizer signal, taken shortly after the 100-minute time in this case, is superimposed on the data plots at 94 to 96 minutes. The nebulizer establishes the vertical

scale calibration as indicated by the upper dashed line. The raw data shown in Figure 10 makes up only three to four points of the Figure 12 plots at the metals turn on time. The very large fly ash transients contribute very little to the one minute integrated data because of their momentary nature. It is also evident from an examination of the data that the threshold detection limit plotted in Figure 9 accurately describes the detectable levels in the 0.2 second data of Figure 10, the 2 second data in Figure 11, and the one minute data of Figure 12

To obtain a single number for each metal for comparison with the results from the EPA reference method, the data were further averaged over the reference measurement (RM) time period as indicated in Figure 12. The results for all the tests are summarized in Table 2. These results differ from those appearing in the DOE report [7] on this EPA field test because the measurements in that report, submitted at the time of the test, were not corrected for zero drift. The early state of development of the R-TiC CEM system for real-time monitoring is evident by the number of missing entries. There was insufficient time prior to the EPA test to bring on line the other metals such as cadmium, mercury, arsenic, and antimony, which were all observed in the laboratory, but needed more work to improve sensitivity in fast flowing aerosols. Also, comparatively little time has been devoted so far to the spectroscopy and data acquisition parts of the R-TiC CEM system. Consequently, as indicated in Table 2, a number of the data records of the metals that were monitored were lost or incomplete due to software or detector array electronics problems. However, the first field test of this technology can be considered successful for producing the results that it did.

Discussion

Test Results

The primary goal of the EPA test was to evaluate the relative accuracy of CEM technologies as compared to the EPA reference, Method 29. In this respect the R-TiC CEM delivered one of the best performances of any CEM technology in a maiden field test. It portends well for meeting EPA's draft Performance Specification for relative accuracy as this technology matures.

Just how well the R-TiC CEM did is given by the analysis in Tables 3-5. The second column in each table lists the R-TiC CEM measurement converted to dry standard cubic meters, the third column the average of the two reference methods upstream of the R-TiC CEM, the fourth column the difference between the R-TiC CEM and RM results in ($\mu\text{g}/\text{dscm}$), and the last column the difference in per cent. A negative difference signifies that R-TiC CEM measurement is lower than the RM measurement. Of the 44 individual tests listed in those tables all but two agree within

Table 2. R-TiC CEM Measured Averaged Metal Concentrations

RM #	Date	Time	Lead ($\mu\text{g}/\text{acm}$)	Chromium ($\mu\text{g}/\text{acm}$)	Beryllium ($\mu\text{g}/\text{acm}$)
1	22 Sept 97	9:36 - 10:37	43.3	20.2	SDL
2	22 Sept 97	11:25 - 2:25	43.8	31.1	SDL
3	22 Sept 97	13:17 - 4:17	36.7	25.9	SDL
4	22 Sept 97	15:15 -16:15	39.6	25.8	33
5	22 Sept 97	17:02 -18:02	44.3	27.7	SDL
6	23 Sept 97	10:01 -11:01	35.2	21.4	SDL
7	23 Sept 97	11:40 -12:40	SDL	SDL	SDL
8	23 Sept 97	13:40 -14:40	54.5	28.0 ^a	SDL
9	23 Sept 97	15:45 -16:45	53.7	32.6	SDL
10	23 Sept 97	17:20 -18:20	40.6	26.7	SDL
11	24 Sept 97	9:40 - 11:10	8.8	9.5 ^a	7.7 ^a
12	24 Sept 97	11:45 -13:15	11.2	11.5 ^a	
13	24 Sept 97	13:45 -15:15	11.1	7.4	8.5
14	24 Sept 97	15:40 -17:10	9.0	6.4	9.1
15	24 Sept 97	17:35 -18:42	12.8	12.2	9.4
16	25 Sept 97	9:20 -10:50	13.1	DEM	13.9
17	25 Sept 97	11:20 -12:50	14.9	DEM	16.3
18	25 Sept 97	13:45 -15:15	14.7	DEM	13.3
19	25 Sept 97	15:35 -17:05	15.1	11.0 ^a	11.3
20	25 Sept 97	17:30 -19:00	11.3	DEM	9.1

SDL: software data loss

DEM: detector electronics malfunction

^a average extrapolated from partial data set

50%. More than two thirds of the measurements for lead and beryllium are within 20% and many are within 10%. Only the results for chromium show a significant systematic offset to lower concentrations. This suggests that there may be a difference in the sack metals concentrations between the upstream RMs and the R-TiC CEM. If this is true then the agreement between the R-TiC CEM and EPA reference method may be better than the present results indicate.

There are a number of observations that suggest that the stack concentrations are different between the upstream location of the reference methods and the downstream location of the microwave plasma. First, the ratio of lead to chromium is different. This is difficult to explain unless the stack concentration is different. The microwave plasma is calibrated by injection, into the ash laden sample stream, of an aerosol of equal concentrations of metals of the same chemistry as those injected into the test furnace. The ratio of metals entering the sample probe is therefore very

Table 3. Lead Results

RM #	R-TiC CEM ($\mu\text{g/dscm}$)	Ref. Methods ($\mu\text{g/dscm}$)	Difference ($\mu\text{g/dscm}$)	% Difference
1	75.0	93.4	-18.4	-19.7
2	75.8	52.2	23.6	45.1
3	63.7	74.7	-11.0	-14.7
4	69.0	67.1	1.9	2.8
5	78.1	42.0	35.6	84.8
6	61.4	93.2	-31.8	-34.4
7	-	95.3	-	-
8	95.4	93.2	2.2	2.2
9	94.3	91.8	2.5	2.7
10	71.9	78.8	-6.9	-8.8
11	15.4	27.8	-12.4	-44.6
12	19.6	23.3	-3.7	-15.7
13	19.5	20.2	-0.7	-3.4
14	15.9	26.0	-10.1	-39.0
15	22.6	27.8	-5.2	-18.8
16	22.8	30.9	-8.1	-26.1
17	26.1	29.4	-3.3	-11.3
18	25.9	31.5	-5.6	-17.8
19	26.6	29.5	-2.9	-9.7
20	20.0	23.5	-3.5	-14.9

accurately measured and is independent of any uncertainty in the nebulizer transport efficiency or in the flowmeter calibration.

Second, if the differences between the R-TiC CEM and RM measurements (4th column of Tables 3-5) are plotted, as in Figure 13, a systematic behavior is evident. At the start of every test day and for every metal, the concentration difference (R-TiC CEM result minus the RM result) has its greatest negative value as compared to later in the day. This behavior is reproducible and is indicated by arrows in Figure 12. There is nothing in the R-TiC CEM system that would vary in this way. The nebulizer transport efficiency is a constant with the standard solution flow and gas flow actively controlled. Any other system changes are automatically accounted for by the span signal. One possible explanation for the systematic difference behavior is a change in the stack between the RMs and microwave plasma every morning, which absorbs more of the metals in the morning, and as a loose deposition coating is built up absorbs less later in the day. Chromium, being the least volatile of the three metals examined here, would be loss more readily, thus accounting for the change in the ratio of chromium to lead.

Table 4. Chromium Results

RM #	R-TiC CEM ($\mu\text{g}/\text{dscm}$)	Ref. Methods ($\mu\text{g}/\text{dscm}$)	Difference ($\mu\text{g}/\text{dscm}$)	% Difference
1	35.0	71.7	-36.7	-51.2
2	53.8	44.9	8.9	19.8
3	44.9	64.2	-19.3	-30.0
4	45.0	56.2	-11.2	-19.9
5	48.5	40.0	8.5	21.5
6	37.4	68.7	-31.3	-45.6
7		71.9	-	-
8	49.0	70.0	-21.0	-31.9
9	57.2	70.8	-13.8	-19.2
10	47.3	63.1	-15.8	-25.1
11	16.6	28.8	-12.2	-42.3
12	20.2	24.8	-4.6	-18.7
13	13.0	22.2	-9.2	-41.4
14	20.4	27.6	-7.2	-25.9
15	21.5	31.3	-10.0	-31.3
19	19.4	29.3	-9.9	-33.8

Third, documented in Figure 7, we observe very large (electronics-saturating) metals signals (concentrations) at end of every test day when the PSI probe was removed and the vacuum break blew off loose deposition from the probe into the stack. The most likely source of this deposition is the stack gas. The PSI probe was freshly reinstalled every morning between the RM locations and the R-TiC CEM.

The R-TiC CEM agreement with the reference method measurements is very close and a 10 to 20 % perturbation in the metals concentration between the RM locations and the microwave plasma would have a significant effect on the present results. It is likely that if a reference measurement were made right beside the R-TiC CEM, agreement would be much closer. It is possible that if the R-TiC CEM system were installed and operated in the immediate proximity to the reference method probe to established the span calibration, then the R-TiC CEM could be accurate to within a few percent for all subsequent monitoring. This, of course, assumes that the plasma efficiency for metals light emission is the same for the calibration aerosol metals and exhaust particulates. If this assumption were true then it would also make the measurements directly traceable to the EPA standard, a necessary requirement for regulatory acceptance.

Table 5. Beryllium Results

RM #	R-TiC CEM	Ref. Methods	Difference	% Difference
	($\mu\text{g/dscm}$)	($\mu\text{g/dscm}$)	($\mu\text{g/dscm}$)	
4	57.5	54.3	3.2	6.0
11	13.5	19.3	-5.8	-30.2
12	-	16.0	-	
13	14.9	14.9	0	0
14	16.0	18.8	-2.8	-14.7
15	16.6	19.5	-2.9	-15.0
16	24.2	22.2	2.0	9.0
17	28.5	23.1	5.4	23.5
18	23.4	23.5	-0.1	-0.3
19	19.9	21.3	-1.4	-6.4
20	16.1	17.4	-1.3	-6.9

If this reasoning is correct then the present results represent a significant advance for the development of multimetals CEMs. They demonstrate for the first time that the EPA goals for accuracy can be achieved and they demonstrate a method by which they are achievable. However, there is a caveat to the calibration method as demonstrated. Only a span calibration was demonstrated. The zero calibration, which is just as important for accurate measurements as indicated in Figure 11, was obtained as an artifact of the testing processes. The feed metals were always turned off between the RM tests, allowing periodic updating of the zero level or background spectrum level for the metals emission signals. It is true the fly ash was present continuously but, because of the data acquisition speed of R-TiC CEM system, when the metals feed was turned off, it was possible to look between the fly ash particulates to determine the true zero level. In an actual furnace facility installation a CEM cannot depend on having the metals turned off for a zero check, therefore a zero check method must be implemented in the CEM system. This should be a realizable goal for future work.

Relative Accuracy

For completeness, a relative accuracy calculation was carried out on the above data. The procedure for calculating the relative accuracy (RA) of a multi-metals CEM to the EPA reference method is documented in the EPA "Performance Specification 10 (PS 10) – Specifications and test procedures for multi-metals continuous monitoring systems in stationary sources" [8]. The equation used to make the comparison is

$$RA = \frac{\left| \bar{d} \right| + \frac{t_{0.975}}{\sqrt{n}} (SD)}{R_{RM}} \quad (2)$$

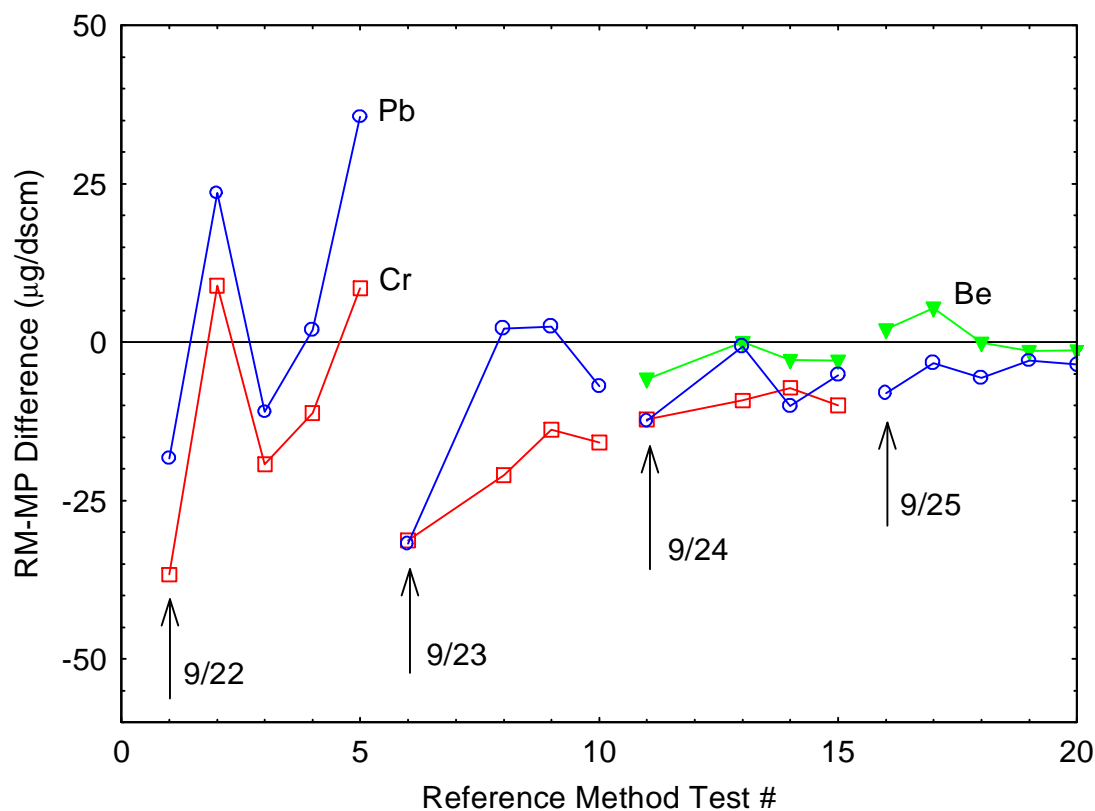


Figure 13. The difference between the microwave plasma and reference method measurements plotted as a function of test number. Arrows point to the first measurement of each day.

where \bar{d} is the mean of the differences between the CEM and reference method measurements (fourth column of Tables 3 – 5), SD is the standard deviation of \bar{d} , n is the number of measurements, \bar{R}_{RM} is the average of the reference measurements (third column of Tables 3 – 5), and $t_{0.975}$ is the t-value of the 2.5% error confidence as given in Table 6.

Table 6. t-values

n	$t_{0.975}$
2	12.706
3	4.303
4	3.182
5	2.776
6	2.571
7	2.447
8	2.365
9	2.306
10	2.262
11	2.228
12	2.201

The resulting relative accuracies for the present field test are given in Table 7. For lead and beryllium the relative accuracies are at or close to the EPA goal of 20%. For chromium the results are consistently off by approximately 40%. However, as the discussion of Figure 13 suggests the relative accuracies may be reflecting a perturbation in the stack metals concentrations between the location of the RMs and the R-TiC CEM.

Table 7. Relative Accuracies

Metal	High Concentration	Low Concentration
Lead	20.5%	30.1%
Chromium	42.8%	42.5%
Beryllium	-	16.4%

Technology Strengths and Limitations

The microwave plasma CEM has many strengths. It is flange-mountable to the exhaust stack and it isokineticly samples a large, undiluted, sample volume on which a large continuous plasma is sustained. It is truly continuous, sampling every particulate and at every instant of time in the sample stream, just as the reference method does. It is capable of fast time resolution and, for Cr, Pb, and Be, already meets EPA's requirement for detection limit. The R-TiC CEM has the combined advantages of near *in situ* operation for sampling a representative volume of stack gas, with the advantage of being just outside the stack to allow access for calibration and for better control of the plasma parameters for maximizing sensitivity. This unique configuration for the R-TiC CEM should eventually allow it to achieve a very high performance capability in both sensitivity and measurement accuracy meeting all the EPA performance requirements.

Another advantage of the R-TiC CEM is that it makes use of relatively inexpensive and reliable components. The magnetron microwave source technology is used in many industrial processes and is mass-produced for home kitchen ovens. It is a mature and reliable technology with long times between failures. The calibration system used an inexpensive pneumatic nebulizer and flow controller that have a long history of successful use in laboratories. The MIT fabricated spectrometer system made use of inexpensive CCD arrays costing one-tenth as much as conventional laboratory-grade systems. Once it is fully developed we expected the R-TiC CEM system to be affordable to all users.

The main limitation of the R-TiC CEM is that additional development is needed to more fully exploit the capabilities of this technology for real-time monitoring of multimetal emissions. The calibration system development is not complete. The performance of the calibration system needs to be more fully evaluated in the laboratory and a zero check method must be provided. Research is needed to determine how representative metals produced from a solution aerosol are of the metals entrained in stack exhaust. More work also remains to be done to improve sensitivity to fast aerosol flows of metals that were not monitored in the present test. In addition, spectrometer and

data acquisition software improvements are needed. There are no fundamental limitations at present to the R-TiC CEM technology and it is expected that all EPA goals for all the RCRA metals will eventually be achieved.

Acknowledgments

The authors gratefully acknowledge the help provided during the testing period by Paul Lemieux and the Acurex personnel at the Environmental Protection Agency National Risk Management Laboratory at Research Triangle Park. We also thank Nina Bergan French (Sky +), Dan Burns (Westinghouse Savannah River), Steve Priebe (INEEL), and Bill Haas (Ames Laboratory) for making this test possible. We're especially grateful to Bill Haas for his review of this manuscript. Finally, we acknowledge the Mixed Waste Focus Area, Office of Science and Technology, U. S. Department of Energy for supporting this technology development.

References

1. P. P. Woskov, D. R. Cohn, D. Y. Rhee, C. H. Titus, J. K. Whittle, and J. E. Surma, Diagnostics for a Waste Remediation Plasma Arc Furnace, Proc. 6th Int. Sym. on Laser-Aided Plasma Diagnostics, Bar Harbor, ME, pp.260-266, and MIT Plasma Science and Fusion Center Report PFC/JA-93-28, October 1993.
2. P. P. Woskov, D. Y. Rhee, P. Thomas, D. R. Cohn, J. E. Surma, and C. H. Titus, Microwave Plasma Continuous Emissions Monitor for Trace Metals in Furnace Exhaust, Rev. Sci. Instrum., Vol. 67, pp. 3700-3707, 1996.
3. D. Y. Rhee, K. Gervais, J. E. Surma, and P. P. Woskov, Detection of Plutonium with the Microwave Plasma Continuous Emissions Monitor, 6 pages, MIT Plasma Science and Fusion Center Report PFC/RR-95-11, 1995.
4. D. D. Smith and R. F. Browner, Measurement of Aerosol Transport Efficiency in Atomic Spectrometry, Analytical Chemistry, Vol. 54, pp. 533-537, 1982.
5. J. D. Jr. And S. R. Crouch, Spectrochemical Analysis, pp. 178 -179, Prentice Hall. Englewood Cliffs, NJ, 1988.
6. H. Takahara, K. Asano, M. Iwasaki, Y. Takamatsu, Y. Tanibata, and T. Suzuki, "Particle Analyzer System", Conference Proceedings 1994, IEEE Instrumentation and Measurement Technology Conference, IEEE Cat. No. 94CH3424-9, p833, 1994.
7. 1997 Performance Testing of Multi-Metal Continuous Emissions Monitors, report prepared for U. S. Department of Energy and Environmental Protection Agency, to be published 1998.
8. U. S. EPA, Revised Standards for Hazardous Waste Combustors, Performance Specification 10 – Specifications and test procedures for multi-metals continuous monitoring systems in stationary sources, 61 FR 17499 - 17502, April 19, 1996.